Journal of the European Ceramic Society 20 (2000) 1311–1318

Severe wear mechanisms in Al_2O_3–AlON ceramic composites

Y. Berriche [a], J. Vallayer [b], R. Trabelsi [b], D. Treheux [b,*]

[a] *Institut de Physique, Université de Annaba, BP 12, 23000, Annaba, Algeria*
[b] *UMR CNRS 5621, Ingénierie et Fonctionnalisation des Surfaces, Ecole Centrale de Lyon, BP 163, 69131 Ecully Cedex, France*

Received 20 April 1998; received in revised form 19 October 1999; accepted 25 October 1999

Abstract

Severe wear mechanisms in Al_2O_3-AlON ceramic composites during their friction against a bearing steel were investigated and analysed by different techniques, mainly transmission electron microscopy (TEM). It was shown that ceramic damages correspond not to a classical intergranular cracking but to a breakdown of alumina–alumina grain boundaries leading to their pull off. Consequently, a new model of the severe wear of ceramics, based on a dielectric approach is proposed. Moreover, the existence of AlON located at such boundaries induces a delaying effect of this damage and seems to participate in the forming and the stability in the contact of a third body essentially constituted by iron oxides.

Keywords: Al_2O_3-AlON; Composites; Electron microscopy; Grain boundaries; Wear

1. Introduction

Al_2O_3–AlON ceramic composites, usually called aluminalon, consists of an alumina matrix (α corindon) into which γ aluminium oxinitride is dispersed. The presence of the γ phase greatly improves both mechanical and tribological properties of alumina. It was shown for example that, for temperature higher than 1000°C, aluminalon exhibits much better properties than pure alumina.[1–4] Hence, the flexural strength (σf) of Al_2O_3–30%AlON composite at $T = 1400$°C is similar to that observed at room temperature, contrary to pure alumina.[3] Moreover, at room temperature, the fracture toughness of aluminalon $(K_{IC})_m$ becomes lower than that of pure alumina, $(K_{IC})_a$, with a rate $R = (K_{IC})_m/(K_{IC})_a = 0.84$. Conversely this rate is equal to $R = 2.93$ at $T = 1400$°C. It is also worth noting that aluminalon hardness is 2185 HV1 compared to 1845 HV1 for pure alumina. On the other hand, from a tribological point of view, fracture toughness and hardness have been shown not to correlate with wear[5–8] and wear surfaces can be classified into two types by focusing on the wear surface profile.[9] Thus, wear which gives a relatively smooth wear surface is defined as "mild wear" and wear which gives a relatively rough wear surface as "severe wear".[9] More precisely, in the mild wear region, the worn surface shows very fine debris and some plastic deformation[6] confirmed by transmission electron microscopy (TEM).[10] The severe wear region is dominated by intergranular fracture and pull out of grains. The distribution of two wear modes was reported in quantitative wear maps by several authors.[6,9] Systematically a steep transition from mild wear to severe wear was reported. It depends on tribological conditions (contact stress, sliding speed, environment, time...) and is associated with the onset of grain boundary fracture.[10] From the microscopic point of view the accumulation of dislocations was believed to be responsible for the time dependent transition to catastrophic wear in ceramics.[10] On the other hand, for aluminalon, it seems that the presence of aluminium oxinitride improves the wear resistance of alumina even for low concentrations.[11]

In this paper, we intend to analyse the wear mechanisms as well as the damaging modes of the ceramic and to bring to the fore the role played by the AlON second phase.

2. Experimental procedure

2.1. Aluminalon elaboration

Aluminalon composites were prepared in "Ecole des Mines de St Etienne" by reactive sintering between alumina (EXAL) and aluminium nitride powders (Starck).

* Corresponding author.
E-mail address: dtreheux@ec-lyon.fr (D. Treheux).

0955-2219/00/$ - see front matter
PII: S0955-2219(99)00294-0

The mixture is hot pressed into a cylindrical crucible. The procedure consists of gradually (30°C/min) increasing the temperature up to about 1800°C where it is stabilised for half an hour under a 40 MPa pressure in order to carry out aluminalon sintering. According to the equilibrium phase diagram of both phases, an oxinitride, of a spinel type γ is formed,[12] whose quantity depends on the chosen initial conditions. For example, an Al_2O_3 molar composition of 90% (of less than 1 μm granulometry and a specific surface of 9 m^2/g) and an AlN molar composition of 10% (of less than 1 mm granulometry and a specific surface of 4.2 m^2/g) give a ceramic consisting essentially of alumina (α) into which the phase (γ) is distributed at about 30%.[13]

2.2. Microstructural analysis

Several techniques were used in order to analyse specimens before and after wear. Damages of ceramics were observed by scanning electron microscopy (SEM) whereas, the nature of crystallographic phases into the contact were investigated by grazing incidence X-ray diffraction (GIXRD). The last technique, transmission electron microscopy (TEM), was used to put into evidence the micro-structure of the ceramic before and after wear. The foils (3 mm discs) were punched from the bulk samples, inside and outside the wear track, mechanically pre-polished parallel to the surface to 60 μm thickness and then sputtered by ionic bombardment. To avoid charging effects by electron beam, one side of the film was covered by an evaporated amorphous carbon.

2.3. Tribological analysis.

Wear tests were carried out using a block-on-ring tribometer (Fig. 1). The ring was a quenched bearing steel cylinder of 35 mm diameter and 65 HRC hardness, rotating against the ceramic block ($12\times12\times8$ mm^3). Prior to any wear tests, the ceramic flat specimens were diamond polished to give a very smooth surface ($R_a = 0.02$ μm). The ring was then grinded directly on the tribometer by friction against a pure alumina block to obtain an average roughness $R_a = 0.08$ μm. All the surfaces were cleaned with acetone in an ultrasonic bath, then rinsed with alcohol and dried in hot air. Wear tests were performed in water with a constant load of 700 N. The rotating speed of the cylinder was 0.36 m/s. According to Ref. 6, such conditions correspond to the severe wear region of alumina.

The wear volume V was determined from the wear track, on the ceramic surface, during the experiments using the following equation[7]:

$$V/L = R^2 \sin^{-1}(b/2R) - b/4(4R^2 - b^4)^{1/2}$$

with (Fig. 1):

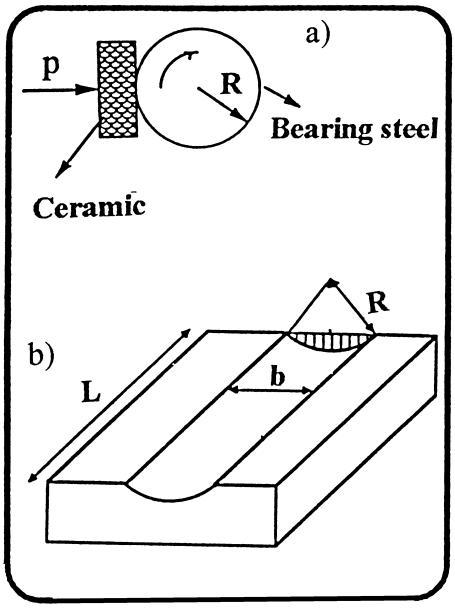

Fig. 1. Schematic representation of the block-on-ring tribometer (a) and of the geometry of the wear track (b).

L: width of the wear track
b: length of the wear track
R: radius of the cylinder.

Both b and L were determined from SEM observation of the wear track.

3. Results and discussion

3.1. Aluminalon microstructure

Fig. 2 shows the (Al_2O_3–30%alon) micro-structure. It is clear that the γ phase, with fair colour, is distributed among an alumina matrix characterised by dark colour. Classical TEM investigations did not reveal the presence of any secondary phase at Al_2O_3–Al_2O_3 or Al_2O_3–AlON grain boundaries under these experimental con-

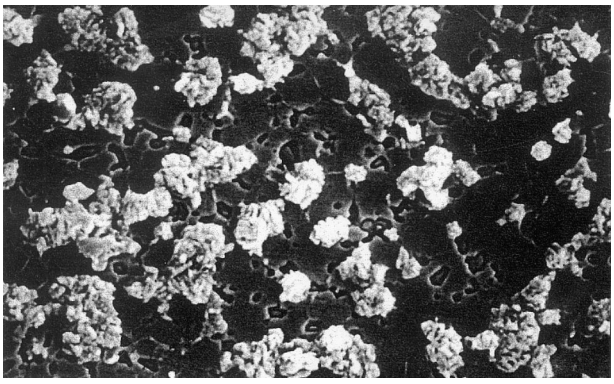

Fig. 2. SEM microstructure of aluminalon after thermal etching.

ditions. It is worth noting (Fig. 3) that AlON grains have various shapes and sizes; some of which whose dimensions are of the order of microns. Moreover, Fig. 4 shows an AlON grain located at alumina grain boundary. They possess an elongated shape whose thickness is of the order of half 1 μm. Such grains present bulk defects in the form of fine platelets with various crystallographic orientations.

3.2. Wear

Wear volumes as a function of the sliding distance are given in Fig. 5 for pure Al_2O_3 and Al_2O_3–30%AlON sintered at $T = 1720°C$. It is clear that the addition of AlON improves the severe wear resistance of alumina.

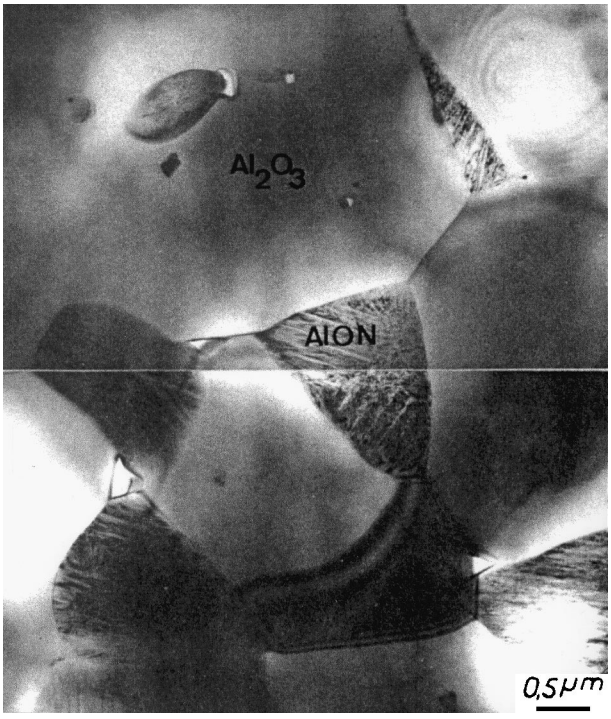

Fig. 3. TEM observation of the distribution of alumina and AlON grain.

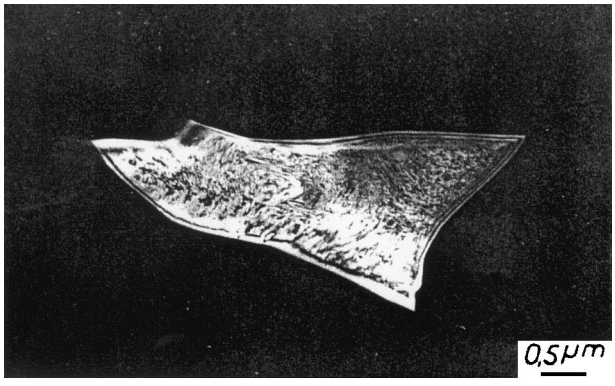

Fig. 4. TEM micrograph of an AlON grain (dark field).

Fig. 6 illustrates the friction coefficient (μ) evolution recorded during the wear test. This curve is characterised by three distinctive periods: (I) a short period where the coefficient increases rapidly, corresponding to surface matching, (II) a stable period around a constant value corresponding to the formation of a dynamic screen (third body)[14–16] caused by wear debris attrition in the contact and (III) an unstable period related to debris elimination and new creation in the contact. In fact the presence of the third body leads to an high friction coefficient level and the decrease in μ is a consequence of the absence of wear debris (third body) in the contact. Therefore, a constant friction coefficient is indicative of an equilibrium state of the third body (II).

3.3. Third body: formation and nature

When the ceramic and the ring are put into contact only the peaks of their asperities get into touch. Hence, three phenomena occur:

1. steel-ring abrasion via micro-cutting into which asperities of ceramic play the role of cutting tools. Steel (α Fe) is locally transferred onto ceramic as proved by GIXRD performed in the wear track after 7 min friction time (Fig. 7);

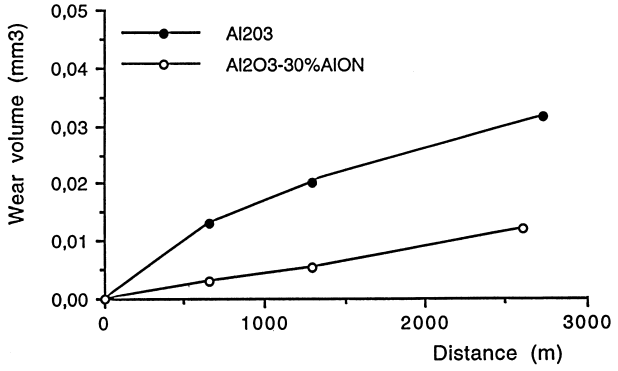

Fig. 5. Wear volume vs sliding distance for pure alumina and Al_2O_3–30%AlON.

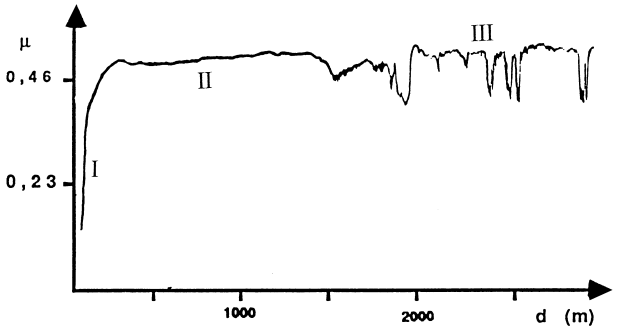

Fig. 6. Evolution of friction coefficient as a function of the sliding distance for Al_2O_3–30%AlON.

2. the iron transferred is then progressively oxided to form iron oxides (Fe_2O_3 and Fe_3O_4) (Fig. 8);
3. wear debris can either be thrown out of the contact or remain in the contact to form the third body. Such a film only has been observed on the ceramic surface as illustrated by Fig. 9.

Hence, the third body, consisting essentially of iron oxides (Fe_2O_3 and Fe_3O_4), (Fig. 8), is formed via an oxidation process of the remaining particles due to dissipated friction energy. The importance of such a third body lies in the separation of both former bodies (ceramic-steel), the decrease of their interaction and their partial protection against wear. The friction changes from steel-ceramic to steel-third body contact. It is interesting to note that this self-protection phenomenon depends on the period of time during which particles remain active. Hence, the wear rate of the ceramic is related to the presence of the third body whose hardness is higher than that of steel.[17] It is well admited that these oxide formation is the predominant process that controls the metal-ceramic wear. It was shown that the third body introduces a film that protects the cracks and limits their propagation.[18] On the other hand, it was reported that the wear resistance of ceramics increases with the oxide film thickness in the contact.[19,20] Finally, it should be noted that the dispersed AlON phase is spread on the surface as ground particles introduced in the third body.

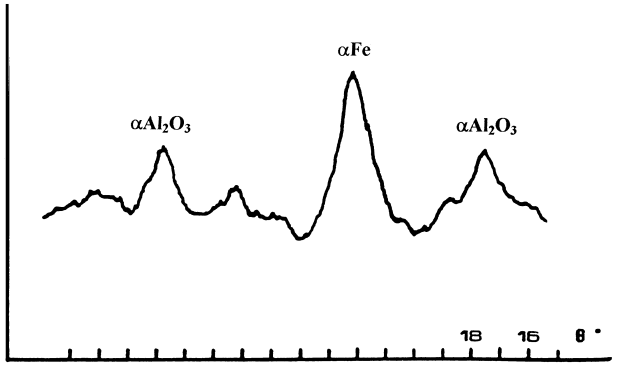

Fig. 7. GIXRD spectrum of the wear track surface after 7 min friction time.

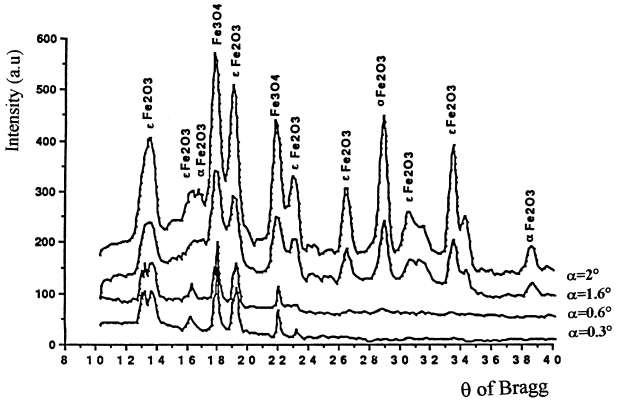

Fig. 8. GIXRD spectrum of the wear track surface after 2 h friction time for different X-ray incidence angles α.

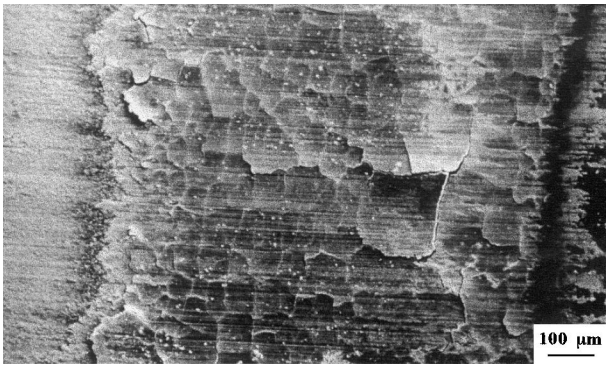

Fig. 9. SEM micrograph of the wear track after 2 h friction time: observation of the third body.

3.4. Observations of ceramic surface after removing of third body

3.4.1. Scanning electron microscopy observations

Wear track observations by scanning electron microscopy after the elimination of the third body show that ceramic damage occurs after alumina grains pull out confirming a severe wear mode. This happens after several successive mechanisms.[7,21] First damages appear as cracks (Fig.10a); grains are initially separated leading at the end to their complete detachment (Fig.10b). Hence, the fracture seems to be essentially an inter-granular process. The presence of AlON phase, as a very thin grain at alumina grain boundaries and triple boundaries, slows down grain pull out, reduces cracks propagation and, hence, ceramic degradation (Fig. 10b). At this stage, all seems to indicate that ceramic damage occurs via intergranular propagation of cracks as reported previously.[6,7,10,21]

3.4.2. Transmission electron microscopy observations

Some aluminalon thin foils, cut off parallel to the worn surface after 30 min friction time, were investigated by a conventional transmission electron microscope. The results thus obtained are illustrated by Fig. 11: it is clear that Al_2O_3–Al_2O_3 grain boundaries, initially free from any phase, are now replaced by a zone (0.2 µm thick) consisting of alumina nanograins (20–30 nm) as shown by diffraction plot taken at the grain boundaries (Fig. 11). It is clear that this boundary destruction leads to the pull out of grains as proved by Fig. 12, onto which the extraction of a grain is obvious. Nevertheless, the nano-crystalline region is maintained around the extracted grain. Thus, these figures agree with SEM observations and confirm the intergranular

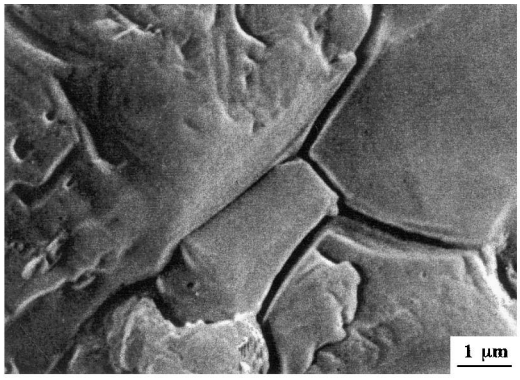

(a)

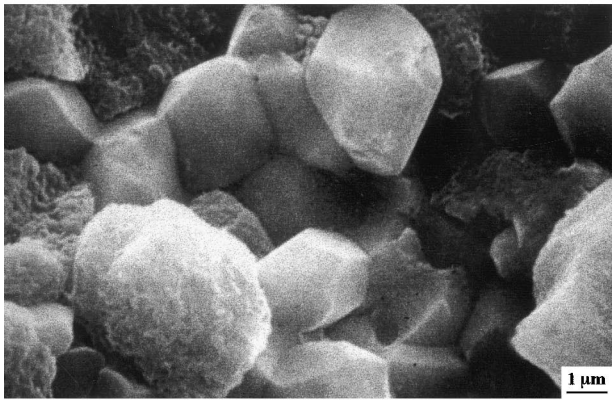

(b)

Fig. 10. SEM observation of the wear track after elimination of the third body after 2 h friction time (a) cracks along alumina grain boundaries; (b) pull out of alumina grains.

aspect of alumina damage. However, the cracking mechanism does not correspond to a classic propagation of intergranular cracks, but to the breakdown of the zone surrounding the grain boundaries, leading to the ejection of alumina grains in the contact.

Such observations, corresponding to an extensive energy (creation of numerous interfaces) can not be explained by simple dislocation pile-ups at grain boundaries resulting in grain boundary cracking as proposed by Barceinas-Sanchez and Rainforth,[10] but can be related to observations of ceramics after electrical breakdown.[22] In this way, it is necessary to consider a form of energy dissipation, too much neglected, i.e. the storage of polarisation energy connected with electrostatic phenomenon identified for a long time[23,24] during contact and friction of insulating materials.

In fact, during movement, when a tangential force is added to the normal load, during movement (friction), non-symmetric and time-dependent deformation of the lattice is observed, leading to possible ionic polarisation and to local variations of the atomic polarisability.[25,26] In other words, friction induces polarisation-depolarisation phenomenon, propagation of a transversal wave in the lattice, instantaneous dipolar field and thus an

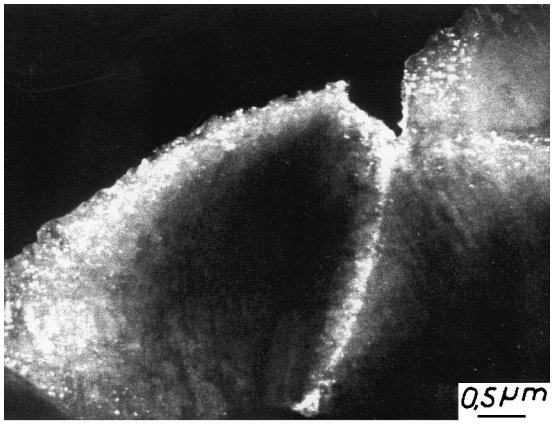

(a)

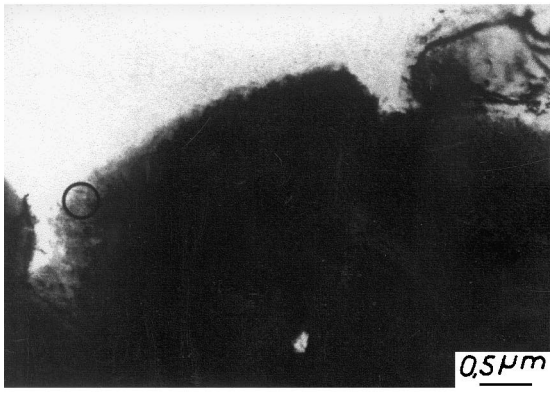

(b)

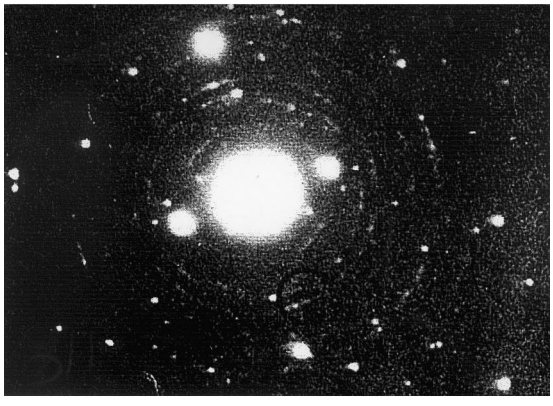

(c)

Fig. 11. TEM micrograph of the Al_2O_3–30% AlON composite after wear in the period II (see Fig. 6.). Breakdown of the alumina near the grain boundary and formation of nanocrystals of alumina as shown by the selected area (O). (a) Dark field (DF); (b) bright field (BF); (c) electron diffraction pattern (α Al_2O_3) of selected area (O).

electric field acting on all the lattice sites. Consequently the energy dE, necessary to the movement, and thus the friction coefficient, has to include a term corresponding to the energy necessary to modify the polarisation in front of the pin. Furthermore, a charge in movement can be trapped on defects (traps) and, in this case, the sample becomes charged. But, the nature of the trap is

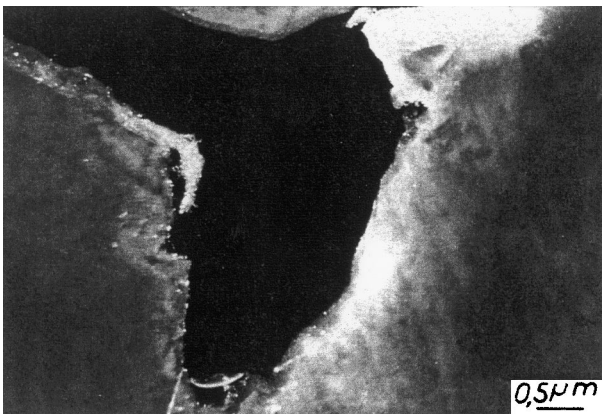

Fig. 12. TEM micrograph of the Al_2O_3-30%AlON composite after wear: observation of the pull-out of an alumina grain as a result of grain boundary breakdown.

not easily discovered. Moreover, a trapping event involves a particular site (impurity, dislocation, grain boundary..., for example) and its surroundings[27–29] and so the trapping energy is expected to be related to the material properties including its elastic constants and electrostriction coefficients. The density of traps and the trap energy distribution also are important questions.[27]

Another major aspect of trapping is the energy stored in a polarised dielectric. The energy is composed of electromagnetic and mechanical contributions with possibly some cross terms. The mechanical energy associated with trapping was introduced on the basis of lattice relaxation accompanying polaron formation[28] or molecular dynamic simulation.[30]

The mechanical energy stored around a trapped charge has been estimated as 5eV/ charge or more[22,28–30.] This energy is considerable and could be compared with the 5eV or so needed to create a defect, typical of bond energy. It is interesting that the maximum elastic energy which can be stored in a solid before plastic deformation or near breakdown (assuming 3.10^6 V/cm and permittivity 10) is on of order 0.5 meV/atom (4 J/cm^3). In other words, a simple calculation showed that 1 trapped charge per 10,000 atoms corresponds to 4 J/cm^3 and could cause breakdown or plastic deformation. In the same way, 1 trapped charge per 1000 atoms corresponds to 40 J/cm^3 and could cause melting of the ceramic.

The relaxation of the polarisation energy associated with trapped charges occurs in two steps. First, charges can be detrapped by the action of an external strain and secondly, the lattice around the location of the charges becomes depolarised, i.e. comes back to its equilibrium configuration. Dissipation of the mechanical energy corresponding to this relaxation mechanism can lead to impact waves producing dielectric flashover, electronic breakdown and mechanical fracture. But it is interesting that without energy localisation, damage is very hard to create and would certainly need some specific site or circumstance.[31]

With regard to tribology, it is clear that contact and friction induce movements of charged particles as shown by triboelectrification and triboemission.[23,24] These charges can be trapped on sites of trapping (pre-existing or formed during friction). Therefore, the tribosystem stores polarisation energy located in special sites. After a given time this polarisation energy can be catastrophically relaxed inducing severe wear. It is thus sensible to study wear not only in mechanical terms but also in dielectric terms.

Moreover if the comparison between electrical and tribological properties is go on, we will have to note that dislocations are formed just as well during friction[10,32] as before electrical breakdown of Al_2O_3 or MgO as proved by Xiang Fu et al.[33] In fact, during injection of charges, some charges in movement are trapped. The main traps for the carriers are impurities. An ample accumulation of trapped carriers lead to the formation of dislocations as proved by TEM: the dislocation density averaged 10^9–10^{10} dislocations/cm^2 whereas the density in virgin crystals was 10^4 dislocations/cm^2.[33] These dislocations can serve in turn as traps for electrons or holes. However, electrically charged, dislocations are mobile under an electric field.

In accordance with the dielectric approach of tribology, the same mechanism can be proposed, i.e. friction induces injection and movement of charges[25,34] which can be trapped on point defects leading to the formation of dislocations. In addition, it is interesting that sites of trapping of charges have been observed recently, inside and outside the friction track, as soon as sliding occurs, during friction of alumina.[34] Probably, such sites were dislocations as observed by[10] and on account of the presence of sites of trapping everywhere in the material (i.e. inside and outside the friction track), the existence of an internal electric field acting on all the lattice sites is confirmed.

In this way, mild wear can be interpreted as the formation of dislocations and the severe wear (detachment of particles) is interpreted as the result of a sudden relaxation of high amount of polarisation energy stored and localised on some special sites i.e. grain boundaries according to TEM observations (Figs. 11 and 12).

4. Proposed model

To sum up, the essence of our model is as follows:

1. friction leads to movement of charges and to polarisation–depolarisation phenomenon inducing an internal electric field;
2. charges in movement are trapped mainly at impurities (in bulk and grain boundaries) leading to the formation of dislocations;

3. all defects (pre-existing or formed during friction) serve as traps for charge carriers (electrons and holes), in movement during friction;
4. in the mild wear region, an equilibrium trapping-detrapping appears without catastrophic effect (severe wear). Dislocations are mobile under the internal electric field involving delocalisation of stored energy except in grain boundaries and when dislocation pile-ups at grain boundaries are formed;
5. in the severe wear region, polarisation energy, locally stored particularly along grain boundaries, can be catastrophically relaxed leading to the breakdown of the grain boundary surrounding;
6. this approach is coherent with the sudden transition from mild wear to severe wear: any circumstance favouring both localised high trapping and sudden detrapping has to exacerbated severe wear (increase of speed, time dependent, instabilities...).

Indeed, such models are in agreement with the classical approach (dislocation formation),[10] recent studies on friction of alumina (formation of sites of trapping inside and outside the wear track)[26,34,35] or wear resistance of zirconias.[8] In the last case, for one type of zirconia (PSZ or TZP) the higher the capacity to trap charges, the bigger the wear and the relaxation intensity depends on the intensity of external solicitations (friction or impact).

5. Conclusion

The wear characterisation of Al_2O_3–AlON composite sliding against bearing steel were studied in the context of the dielectric approach of the ceramic tribology of ceramics.

The ceramic damages, analysed by TEM are well located at alumina–alumina grain boundaries, but such damage does not correspond to conventional crack propagation. It is obvious that a transformation of bulk alumina near by grain boundaries occurs inducing the formation of alumina nanocrystals.

This intergranular breakdown could be explained by the local storage and then release of polarisation energy along grain boundaries, occurring during friction. We proposed that this polarisation energy is connected to trapping of charges on defects pre-existing (point defects, grain boundaries...) or created by friction (dislocations). Such trapping of charges can be responsible to formation of high density of dislocations by electro-mechanical effect as shown both before electrical breakdown[33] and during friction of ceramics.[10,32]

Both dislocation pile-ups and trapping of charges at grain boundaries lead to an high localisation of charges, and thus of polarisation energy, which can induces severe wear if the relaxation of the stored energy occurs on account of friction conditions.

The addition of AlON, in dispersoid form, in the alumina matrix improves the wear resistance of ceramic-steel friction. At first the inter–granular location of AlON seems to limit the localisation of polarisation energy (charge flow or storage in bulk AlON) and thus the pull out of grains. Then AlON stabilise in the contact the third body, essentially constituted of iron oxides. Such a body protects partially the ceramic from damaging.

Acknowledgements

The authors wish to thank to D. Gœuriot and P. Gœuriot for the elaboration of ceramic composites in Ecole des Mines de St Etienne (France).

References

1. Goeuriot, D., Réactivité, frittage et caractérisation de céramiques dans le système alumine-oxynitrure d'aluminium g et nitrure de bore. Thèse d'état ès Sciences Lyon I, juin 1987.
2. Launay, D., Goeuriot, P., Thevenot, F., Orange, G., Fantozzi, G. and Tréheux, D., L'aluminalon nouvelle céramique composite. *L' industrie céramique*, 1985, **798**(10), 708.
3. Goeuriot-Launay, D., Goeuriot, P., Thevenot, F., Orange, G., Fantozzi, G., Tréheux, D. and Trabelsi, R., Effet d'une dispersion d'alumine sur les propriétés de l'alumine. *Silicates industriels*, 1989, **1–2**, 3.
4. Launay, D., Orange, G., Goeuriot, P., Thevenot, F. and Fantozzi, G., Reaction sintering of an Al_2O_3–AlON composite. Determination of mechanical properties. *J. Mater. Sci. Letters*, 1984, **3**, 890–892.
5. Kim, S. S., Kato, K., Hokkirigawa, K. and Abe, H., Wear mechanism of ceramic materials in dry rolling friction. *J. Trib*, 1986, **108**, 522.
6. Wang, Y. S., Hsu, S. M. and Munro, R. G., Ceramics wear maps: alumina. *J. Soc. Trib. Lubrication Engineers*, 1991, 63–69.
7. Trabelsi, R., Orange, G., Fantozzi, G., Homerin, P. and Thevenot, F., Relationship between mechanical properties and wear resistance of alumina zirconia ceramic composites. *J. Lubrication Engineers, Tribology Trans*, 1989, **32–1**, 77–84.
8. Médevielle, A., Tréheux, D. and Thévenot, F., Wear resistance of zirconias:dielectrical approach. *Wear*, 1997, **213**, 13–20.
9. Kato, K. and Adachi, K., Wear maps of advanced ceramics. In *9th Cimtec World Ceramics Congress. Ceramics Getting into 2000's. Part A*, ed. P. Vincenzini. Techna Srl., 1999 pp. 477–487.
10. Barceinas-Sanchez, J. D. O. and Rainforth, W. M., On the role of plastic deformation during the mild wear of alumina. *Acta. Mater*., 1998, **46**(18), 6474–6483.
11. Goeuriot-Launay, D., Goeuriot, P., Thévenot, F., Orange, G., Fantozzi, G., Tréheux, D. and Trabelsi, R. Friction, wear resistance and mechanical properties of an aluminium oxynitride composite. In *6th CIMTEC Milan June (1986) High Tech. Ceramics, ed.* P.Vincenzini Elsevier; Amsterdam, 1987.
12. Mc Cauley, J. W. and Corbin, N. D. In *Progress in Nitrogen Ceramics*. Ed. F.L. Riley. Nijhoff M. Publishers, La Hague, 1983. p. 111.
13. Goeuriot-Launay, D., Goeuriot, P. and Thévenot, F., Science of Ceramics 14, ed. G. B. D. Taylor. Butler et Tanner, London, 1987, p. 181.
14. Godet, M., The third body approach: a mechanical point of view. *Wear*, 1984, **100**, 437.

15. Godet, M., Extrapolation in tribology. *Wear*, 1982, **77**, 29–44.
16. Lancaster, J. K., Play, D., Godet, M., Verall, A. P. and Waghorne, R., Third body formation and the wear of PTFE fibre based dry bearings . *J. Lub.Techno*, 1980, **102**(2), 236–246.
17. Peterson, M. B. and Lee, R., *Wear*, 1964, **7**(4), 334.
18. Godet, M. and Berthier, Y., Mécanique de la tribologie, application aux céramiques. *L'industrie céramique*, 1986, **808**(9), 565–568.
19. Mehan, R. L. and Hayden, S. C. *Wear* 1981–1982, **74**, 1213–1227.
20. Williams, J. A. & Eve, R. W., Int. Conf. on Tribology, London, 1987, p. 183.
21. Berriche, Y. and Tréheux, D. Role d'ajouts (BN, Y_2O_3, SiC) sur le comportement tribologique du composite Al_2O_3-AlON. *La Revue de Métallurgie CIT/ Science et Génie des Matériaux* 1998, pp. 691–697.
22. Blaise, G. and Le Gressus, C., Mise en évidence d'un claquage des isolants associé à la déstabilisation d'une charge d'espace localisée. *C. Rendu Acad SC*., 1992, **314**(2), 1017–1024.
23. Harper, W. R. Contact and Frictional Electrification. Oxford University Press, 1967.
24. Nakayama, K. and Hashimoto, H., Triboemission of charged particles and photons from wearing of ceramic surfaces in various gases. *Tribology Trans*, 1992, **35**(4), 643–650.
25. Fayeulle, S., Bigarré, J., Vallayer, J. and Tréheux, D. Effect of a space charge on the friction behavior of dielectrical materials. *Le Vide, les couches minces* suppl. 1995, 275, 74–83.
26. Tréheux, D., Bigarré, J. and Fayeulle, S., Dielectric aspects of the ceramic tribology. *9th Cimtec World Ceramics Congress. Ceramics Getting into 2000's. Part A*, ed. P. Vincenzini. Techna Srl., 1999, pp. 563–574.
27. Damame, G., Le Gressus, C. and De Reggi, A. S., Space charge characterization for the 21th. *Century. IEEE Trans. on Dielectric and Electrical Insulation*, 1997, **4**(5), 558–584.
28. Blaise, G. and Legressus, C., Charge trapping-detrapping process and related breakdown phenomena. *IEEE Trans. on Electrical insulator*, 1993, **27**, 472–479.
29. Blaise, G., New approach to flashover in dielectrics based on a polarization energy relaxation mechanism. *IEEE Trans. on Electrical insulator*, 1993, **4**(28), 437–443.
30. Rambaut, C., Oh, K., Jaffrezic, H., Kohanoff, J. and Fayeulle, S., Molecular dynamics simulation of electron trapping in sapphire. *J. Applied Phys*., 1997, **81**(3), 3263–3267.
31. Stoneham, A. M., Electronic and defect process in oxides: the polaron in action. *IEEE Trans. on Dielectric and Electrical Insulation*, 1997, **4**(5), 604–613.
32. Hockey, B. J., Plastic deformation of aluminium oxide by indentation and abrasion. *J. Am. Ceram. Soc*., 1971, **54**(5), 223–231.
33. Xiang-Fu, Zhong, Chen-Fu, Shen, Song Liu, Y. and Chen Renjun, Zhang, Model for radiation induced degredation of αAl_2O_3 crystals. *Physic Review B*, 1996, **54**(1), 139–143.
34. Fayeulle, S., Berroug, H., Hamzaoui, B., Tréheux, D. and Le Gressus, C., Role of dielectric properties in the tribological behaviour of insulators. *Wear*, 1993, **162–164**, 906–912.
35. Berroug, H., Fayeulle, S., Hamzaoui, B., Tréheux, D. and Le Gressus, C., Effect of X ray irradiation on the properties of insulators. *IEEE Trans. on Electrical Insulator*, 1993, **28**(4), 528–534.